IMPACT OF A DRY BED SURGE AGAINST STRUCTURES WITH AND WITHOUT OPENINGS

DAVIDE WÜTHRICH[(1)]

[(1)] Laboratoire de Constructions Hydrauliques (LCH), Ecole Polytechnique Fédérale de Lausanne (EPFL), Lausanne, Switzerland, davide.wuthrich@epfl.ch

ABSTRACT

Tsunamis, Impulse waves and the sudden collapse of dams are rare phenomena, but highly destructive. Nevertheless recent events showed that structures with openings can effectively reduce impact forces, ensuring people's safety and limiting reconstruction costs. The present experimental study systematically investigates the impact of a dry bed surge against a free standing structure with various degrees of porosity, measuring forces and moments in all directions. For the impervious scenario, results showed the absence of an initial overshot and a good agreement with the classical hydrodynamic force computed as a function of the momentum flux. Structures with openings showed lower upstream water levels resulting in a reduced horizontal load. This was proved to be linearly proportional to the porosity value and the application point of the force was between 75 and 100 % of the maximum wave height, independently from the geometry. Vertical forces are given as the sum of buoyancy and the weight of water, presenting the highest values for porosities between 17 and 34 %.

Keywords: Tsunami; impulse wave; dam-break wave; impact forces; openings.

1 INTRODUCTION

Extreme natural events such as tsunamis, floods and storms are occurring more often, exposing human to severe hazardous consequences. Tsunamis and impulse waves, induced by landslides into water reservoirs, can generate extreme damage to buildings and infrastructures located near the shore along with often catastrophic loss of human lives. A strong similarity was proven between tsunami induced bores and hydrodynamic waves produced by the sudden collapse of a dam (Chanson, 2006). Some previous tragic events took place in Sumatra Island (Indonesia, 2004) and in Tōhoku (Japan, 2011). According to the World Bank, these events combined produced over 300'000 deaths and damages for over 240 billion USD. Nevertheless, these events showed that engineering and coastal planning measures can be effective to ensure people's safety and reduce reconstruction costs. Furthermore a properly designed building can represent a vertical shelter which can save people's lives (Figure 1a). The role of engineers and researchers is therefore to develop and design infrastructures able to withstand natural disasters and protect human lives.

(a)  (b) 

Figure 1. (a) Example of tsunami-structure interaction during the Indian Ocean tsunami (2004) [MThompson]; (b) Example of porous structure: Port building in Ofunato Chock et al. (2013) [Robertson].

In the past the impact of hydrodynamic waves on structures was considered too rare and the resulting impact forces were typically neglected in the design process. A few studies on the impact of waves against structures were carried out to characterize and estimate this extreme hydrodynamic loading. However, the large amount of empirical or semi-empirical formulas available and their significant scattering suggested that the behavior of structures under such extreme loading is not yet fully understood. Post-tsunami forensic engineering surveys have shown that some structures behave better than others; moreover, buildings with openings seem to resist better under hydrodynamic impact (Figure 1b). Previous studies proved that a specific design can significantly decrease the load on the free-standing structure. The investigation of a tsunami

resistant house in Sri Lanka designed by the Harvard School of Architecture in collaboration with MIT showed that the allowance of a flow through the building resulted into a better performance of the structure compared to the conventional design (Thusyanthan and Madabhushi, 2008). Van de Lindt et al. (2009) proved that just by opening windows and doors the load was reduced by 60%. Furthermore, structures with opening configurations of 25 and 50% reduced the hydrodynamic force by 15-25% and 30-40% respectively (Lukkunaprasit et al., 2009a; Chinnarasri et al., 2013). Hartana and Murakami (2015) compared some experimental tests to numerical simulations for porosity values of 40 %. Nevertheless, the influence of porosity and openings on the resulting hydrodynamic force remains mostly unknown and forces it to be difficult to estimate.

2 EXPERIMENTAL SET-UP

The present study is based on an experimental approach. Tests were carried out in a large-scale facility at the Laboratory of Hydraulic Constructions (LCH) at the Ecole Polytechnique Fédérale de Lausanne (EPFL), in Switzerland. Wave formation was achieved through the vertical release of a known water volume from an upper reservoir, through multiple pipes into a lower tank linked to a horizontal channel (Figure 2). A similar technique was previously used by Chanson et al. (2002), Lukkunaprasit et al. (2009b), Meile et al. (2013) and Wüthrich et al. (2017). The wave propagated on a horizontal smooth channel with a total length of 15.5 m and a width (W) of 1.4 m. The roughness of the channel bottom was calculated through steady state experiments to a Darcy-Weissbach friction coefficient of f = 0.021. The produced bores were similar to classical dam-break waves where nowadays it is considered a more appropriate technique to reproduce bores and surges propagating inland, as tsunamis hardly produce a solitary wave (Yeh et al., 1996; Chanson, 2006; Madsen et al., 2008; Nistor et al., 2009; Nouri et al., 2010). The flexibility of the experimental set-up allowed to produce dry bed surges with various equivalent impoundment depths (d_0), representing the first incoming wave. Different surges with different hydrodynamic properties were produces, mainly in terms of wave height (h) and wave front celerity (U). The time-histories of the wave height in different locations of the channel were measured using 7 Ultrasonic distance Sensors (US) located at x = 2.00, 10.10, 12.10, 13.10, 13.35, 13.60 and 13.85 m, sampled with an acquisition frequency of 12.5 Hz. Signal post-processing allowed to compute the wave front celerity (U) of the propagating wave averaged on the entire channel.

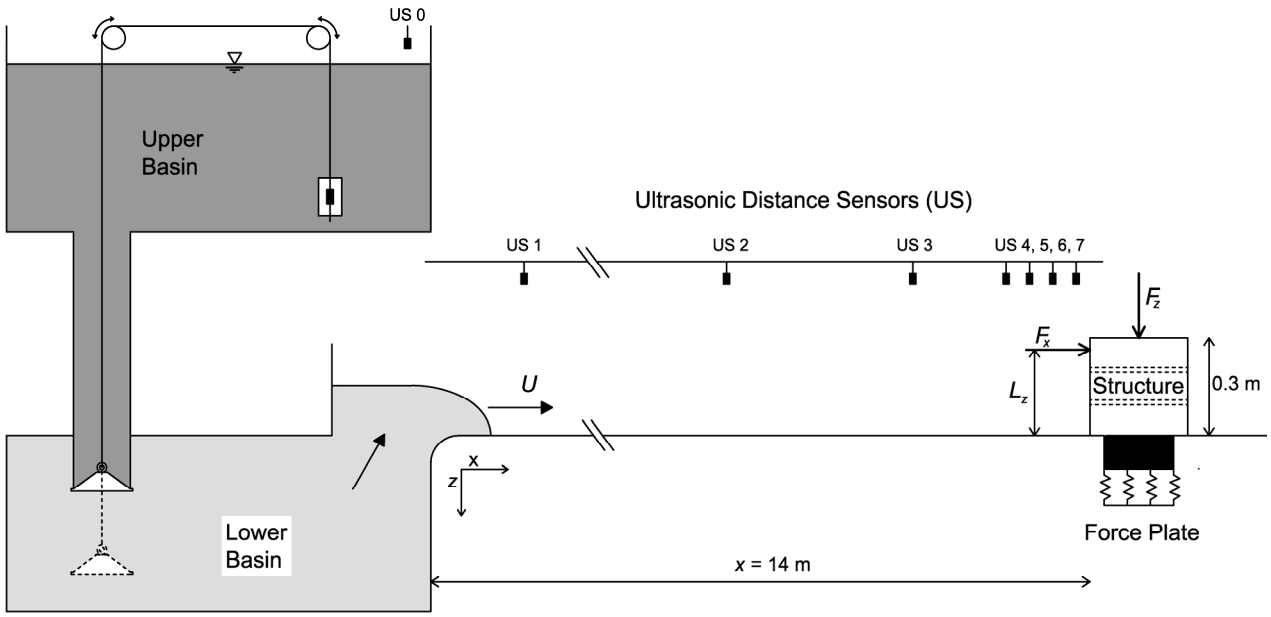

Figure 2. Experimental set-up used to produce dry bed surges through a vertical release technique.

The tested structures were located at a distance of 14 m from the channel inlet and had a width (B) of 0.3m, resulting into a blockage ratio $\beta = W/B = 4.7$. This value was sufficiently high to limit major side effects. The structures were made of aluminum cubes with a thickness of 10 mm and they were designed to be completely rigid, ensuring that the structure's response could be neglected. Numerical simulations of push-over tests allowed to calculate a stiffness values ranging between k = 2.2 - 1.8 · 10^8 N/m for all tested structures. These structures corresponded to buildings with height and width of 9 m if a Froude scaling ratio of 1:30 is assumed. This corresponded to residential houses commonly observed in coastal zones exposed to tsunami hazard. As shown in Figure 2, the structures were installed on a dynamometer force plate (AMTI MC6-1000) which recorded the time-history of the impact forces and moments, including surge and drag components, with an acquisition frequency of 1 kHz. The installation of two floors inside the buildings allowed to measure the vertical component of the force induced by buoyancy and the weight of the water flowing

through the structure. The spatial and temporal development of the phenomenon was captured by means of a high speed cameras.

3 METHODOLOGY

The objective of this research project was to systematically evaluate the effect of building openings on the resulting hydrodynamic load via laboratory experiments. A list of the tests performed for the present study is presented in Table 1 along with the main characteristics of each experiment. A test without structure was also performed to characterize the hydrodynamic behavior of the wave. This corresponded to the P = 100 % scenario. In this paper, H corresponds to flow height with the structure, whereas h is the wave height without the structure; F_x is the total horizontal force applied by the incoming wave against the structure, measured at the foundation. The surface porosity P is defined as the ration between the openings (A_o) and the building surface (Eq. [1]):

$$P = \frac{A_o}{B^2} \quad [1]$$

Table 1. Experimental program.

Test	Porosity P [%]	Bed condition	Impoundment depth d_0 [m]	Wave front celerity U [m/s]	Height h_{max} [m]	Height H_{max} [m]	Force $F_{x,max}$ [N]
1	0	dry	0.63	3.07	0.178	0.519	196.6
2	17	dry	0.63	3.08	0.178	0.543	166.9
3	34	dry	0.63	3.08	0.178	0.548	140.7
4	60	dry	0.63	3.08	0.178	0.507	84.3
5	100 (no structure)	dry	0.63	3.07	0.178	-	-

A good repeatability for all tests was observed, but herein not showed. The structures were not submerged for any incoming wave; however some initial run-up splashes were higher than the building rooftop (Figure 3). The wave front celerity U was in the range predicted by FEMA 55 (2000) and CCH (2000) for the given impoundment depths.

4 VISUAL OBSERVATIONS

The impacts of the propagating waves on the free standing structure were recorded through high speed cameras and GoPro videos. The impact mechanism on impervious structures for waves with different hydrodynamic properties was previously discussed by Wüthrich et al. (2016). Herein all tested scenarios showed crown-shaped splashes and run-up heights higher than the structure, as shown in Figure 3, however this was only limited to the first seconds. After the impact no overflow was observed for any configuration. For structures with openings the water was able to flow through the structure resulting into an interaction between the incoming surge and the building. Initially the water flowing through the structure only affected the first floor, however with the increase of the upstream height, the second and third floors were also eventually inundated. Being the sides open, a portion of the water entering from the front side left the building through these openings, resulting into an interaction with the flow around the structure (Figure 3b).

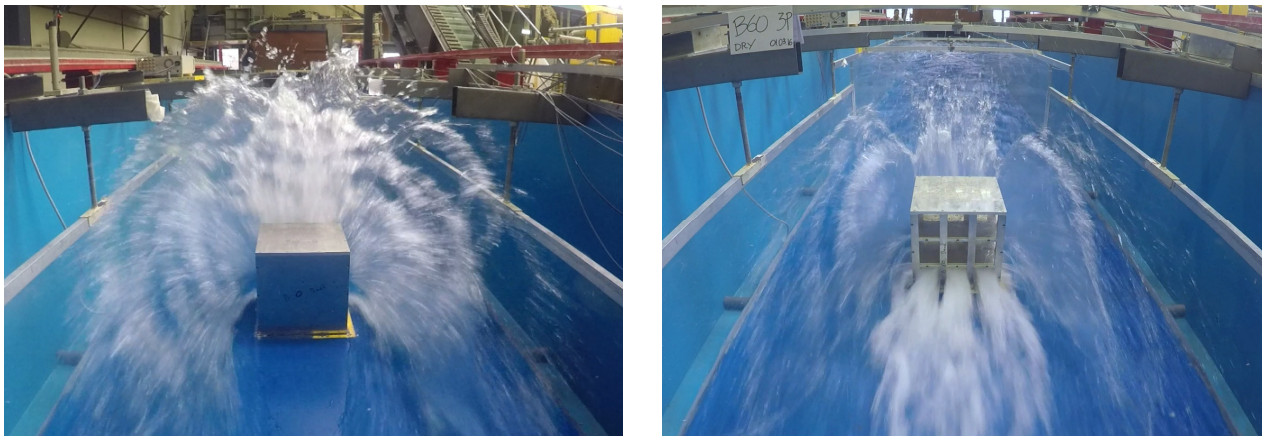

Figure 3. Wave impact against: (left) impervious (P = 0 %) and (right) porous (P = 60%) structure for a dry bed surge with equivalent impoundment depth d_0 = 0.63 m and front celerity U = 3.08 m/s.

Measurements carried out with US probes allowed to measure the run-up heights during the impact; these are presented in Figure 4. One can notice similar run-up heights during the impact (H_{max}, Table 1) for all tests, nevertheless on the upstream side, lower water levels were recorded for larger porosity values. For all

scenarios a fluctuating behaviour was observed, attributed to the presence of a recirculating roller on the upstream side of the building. The intensity of the roller was more important for the impervious structures. Some similar results in terms of visual observations of experimental tests and comparison with numerical simulations were carried out by Hartana and Murakami (2015) for structures with openings and internal slabs.

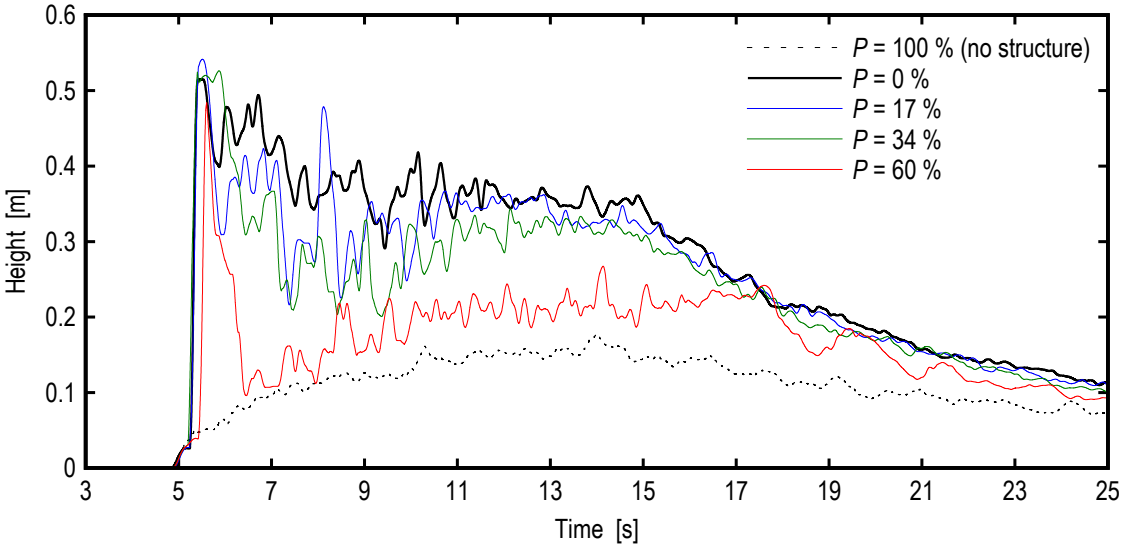

Figure 4. Ultrasonic distance sensors (US) measurements of run-up heights *H* for various porosity values.

5 LOAD ANALYSIS

The research focused on the effect of building openings on the hydrodynamic loading. The estimation of forces is important to design structure that will withstand the impact of the incoming tsunami. The data obtained for the structures with openings was compared with the reference impervious structure (P = 0 %). Both horizontal forces and vertical forces were considered in the present study.

5.1 Horizontal forces on impervious structures (P = 0%)

During a wave impact, horizontal forces F_x are predominant and their estimation is essential to guarantee the survival of the structure. This is important because buildings are rarely dimensioned to resist horizontal forces, unless they are located in seismic areas. The estimation of the horizontal force produced by a flow against a structure can be predicted using Morison's Equation, taking into account a hydrodynamic (or drag) component and an inertia component. For tsunamis, due to their long periods, the inertia component becomes important only at the leading edge, when the wave impacts the structure: this is often called *surge force*. The hydrodynamic component in the x direction $F_{x,D}$ can be computed using the expression presented in Eq. [2]:

$$F_{x,D} = \frac{1}{2}\rho C_D B h v^2 \qquad [2]$$

where ρ is the water density, B the structure width, h the flow height and v the flow velocity. A drag coefficient C_D is commonly used, whose value depends on the geometry and on the flow conditions.

In the present study, the total horizontal force F_x produced by a dry bed surge impacting against an impervious structure was measured by means of a dynamometric force plate with a frequency of 1 kHz. The diagram obtained is presented in Figure 5, where one can notice a constant increase of the load until a force oscillating around a constant value was reached. Such behavior was consistent with previous studies, including, among others, Cross (1967), Ramsden (1996), Arnason et al. (2009), Lukkunaprasit et al. (2009b) and Nouri et al. (2010). In the present case, no force overshot due to surge component was observed during the impact, as previously discussed by Ramsden (1996) and Yeh (2007).This is probably due to the mild slope of the incoming surge. It is therefore reasonable to conclude that for a dry bed surge the inertia component (surge force) can be neglected.

In agreement with what was visually observed, after the impingement, the flow became quasi-steady due to the surge's long period and the estimation of the force could be obtained through the classical hydrodynamic equation presented in Eq. [2]. It is important to point out that the maximum hydrodynamic force $F_{x,D,max}$ does not occur when both h and v are maximal, but when the momentum flux per unit width ($M = hv^2$) is maximum, i.e. $M_{max} = (hv^2)_{max} \neq h_{max}v^2_{max}$ (Yeh et al., 1996; Yeh, 2007). It was shown by Wüthrich et al. (2017) that the depth-averaged profile velocity behind the wave front (V_m) decreased with time with nonlinear behavior. The product of a decreasing V_m with an increasing h lead to a maximum momentum flux occurring around 2/3 of h_{max}.

The behavior of the measured force is plotted in Figure 5 and compared with some formulae commonly found in literature. This study confirms what was previously observed by Ramsden (1996), that the actual measured force F_x was less than the force computed using the run-up height H assuming hydrostatic conditions ($F_x < F_{x,H}$). The measured force was also higher than the force computed with the wave height h without the structure ($F_x > F_{x,h}$). For the present study, the best approximation was found with the hydrodynamic force computed using the depth-averaged profile velocity V_m behind the front, as presented in Eq. [3]:

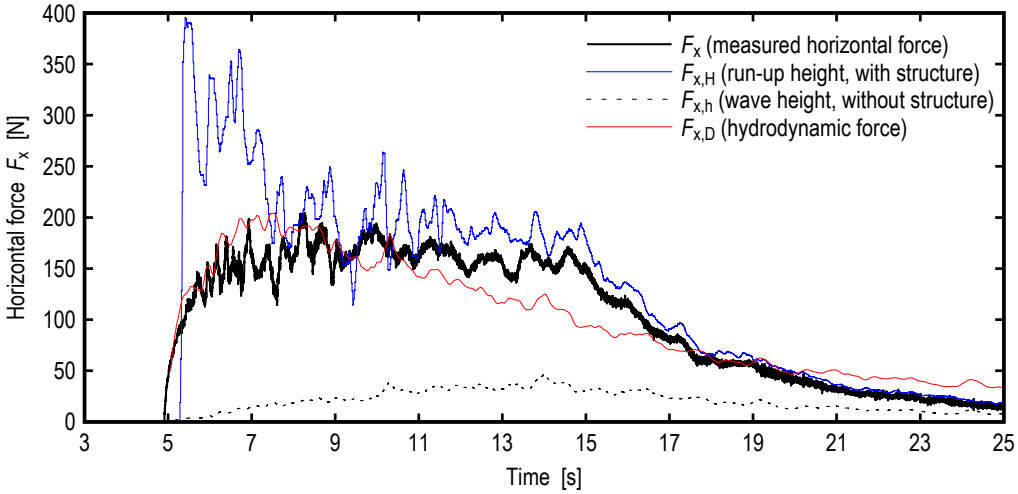

Figure 5. Comparison of force diagram, F_x, for the reference impervious structure (P = 0%) with existing formulae in literature.

$$F_{x,D} = \frac{1}{2}\rho C_R BM = \frac{1}{2}\rho C_R Bh V_m^2 \qquad [3]$$

where h is the wave height measured without the structure, B the structure width and V_m the depth-averaged wave profile velocity, calculated using the expression presented in Wüthrich et al. (2017). Similarly to Arnason et al. (2009), herein a resistance coefficient C_R = 2 was used. The advantage of using a resistance coefficient C_R instead of a drag coefficient C_D was to take into account the hydrostatic pressure difference between the back and the front of the structure, which may contribute to a portion of the measured impact force. The good agreement observed in Figure 5 proved that the force was therefore proportional to the Momentum flux $M = hV_m^2$. One can also notice an underestimation of the force in the post-peak region (t > 11 s); this is because all parameters in Eq. [3] refer to the wave without the structure, whose phenomenon is associated with a shorter duration.

5.2 Horizontal Forces on Porous Structures

Once the force produced against the impervious structure was characterized, the following step was to investigate the loads produced on the porous structures. Coastal structures are seldom impervious cubes and most often are characterized by openings such as windows and doors. In the present study four configurations were chosen with total values of P = 0, 17, 34 and 60 %. The first porosity value (17 %) was chosen to represent small windows, the second (34 %) large windows and the last (60 %) only the load-bearing structure. Surface porosity was uniformly distributed and equally applied on all four vertical surfaces of the structure, simulating an isolated building. Horizontal plates were inserted to simulate the slabs between the floors and the roof (Figure 2). Sketches of the geometries tested are presented in Figure 6.

The time-histories of the four horizontal forces F_x measured for a wave with the same initial release conditions are plotted in Figure 7. One can notice that the overall behaviour was similar for all scenarios: after an initial increase of the force, the load stabilized around a constant value before decreasing once the wave had passed. As previously discussed, for dry bed surges no initial overshot was observed for any configuration. Major differences could be observed in terms of the vertical stretch of the curve, with large porosities having lower values. This was attributed to the presence of openings on the structure, reducing the inundation depth in front of the building, as previously observed by Hartana and Murakami (2015). Moreover, porous structures had a less steep force increase resulting into a slower and milder loading condition.

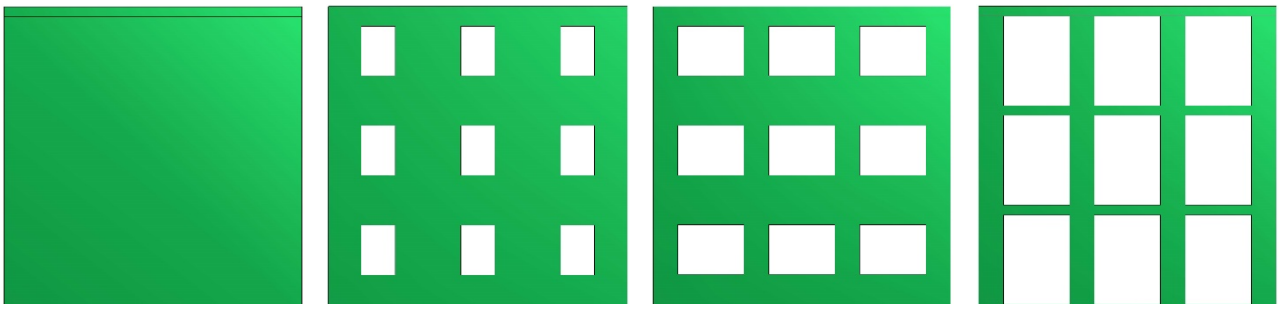

Figure 6. Buildings configurations tested in the present study, with identical geometry on all four sides.

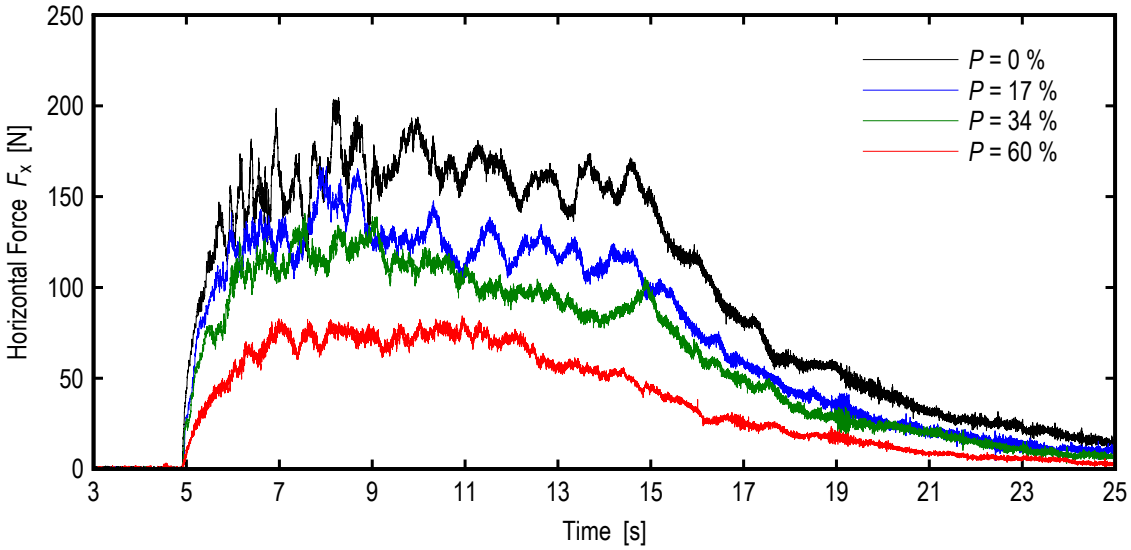

Figure 7. Horizontal force F_x diagrams obtained for a dry bed surge for the same initial release conditions.

For all tested scenarios shown in Figure 7, the absolute maximum $F_{x,max}$ was plotted as a function of the surface porosity P and normalized using the maximum horizontal force measured for the reference impervious structure $(F_{x,max})_{P=0}$. Results are presented in Figure 8, where a linear behavior can be identified. It is hypothesized that the horizontal force F_x is zero in the absence of the structure (P = 100 %), allowing to obtain a more precise regression. These preliminary findings suggest that the reduction of the horizontal load is proportional to the surface that is exposed to the incoming wave, as shown in Eq [4]:

$$F_{x,\max} \cong \left(F_{x,\max}\right)_{P=0} \cdot (1 - P) \qquad [4]$$

where $F_{x,max}$ is the maximum horizontal force, $(F_{x,max})_{P=0}$ is the maximum horizontal force measured for the impervious configuration (P = 0) and P the surface porosity of the structure. These findings validated the preliminary conclusions drawn by Lukkunaprasit et al. (2009a), who suggested using a linear approximation in lack of experimental tests.

Once the magnitude of the force was defined, designers must know at which height of the structure this force should be applied. Through the moment around the y-axis M_y and the horizontal force F_x it was possible to compute the lever arm L_z, i.e. the application point of the force from the channel bottom, through Eq. [5]:

$$L_z = \frac{M_y}{F_x} \qquad [5]$$

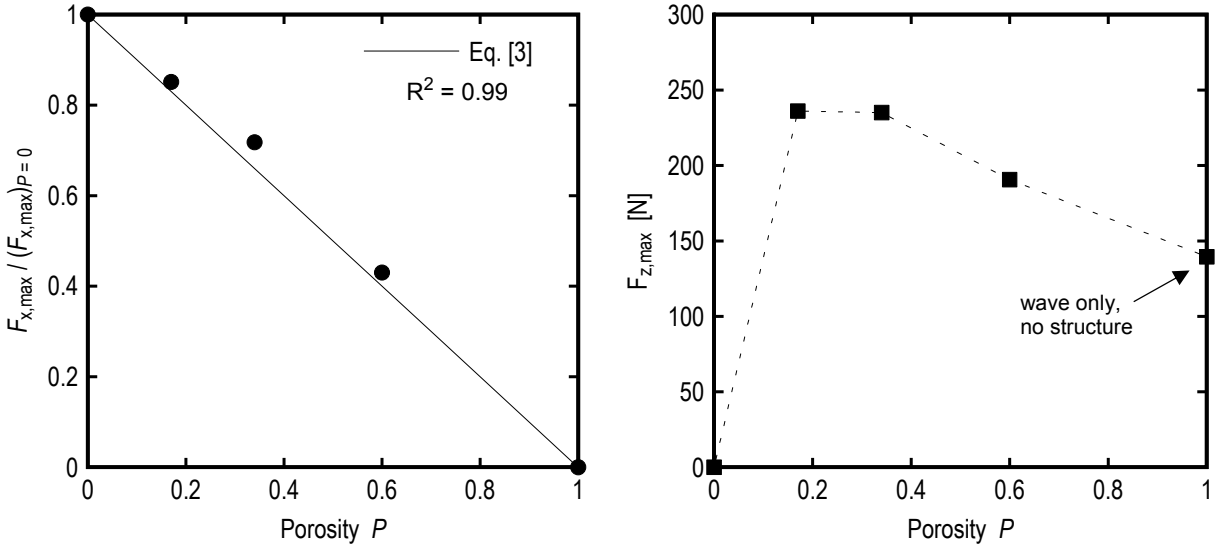

Figure 8. Maximum horizontal force F_x and vertical force F_z as a function of surface porosity *P.*

The results are plotted for all configurations in Figure 9, normalized using the maximum wave height h_{max} measured without the structure. At impingement, a different behavior can be observed for the tests with larger porosity values, where a minor overshot can be identified. During the hydrodynamic process following the impact, the lever arm L_z was similar for all scenarios and it corresponded to distances between 75 to 100% of the maximum wave height h_{max} measured without the structure. It is important to point out that the actual water level on the upstream side of the building is highly influenced by the presence of the structure, leading to run-up heights of H greater than h_{max}, as previously shown in Figure 4. These findings pointed out that the surface porosity of the structure does not significantly influence the application point of the force F_x, which can be assumed constant for all configurations (Figure 9).

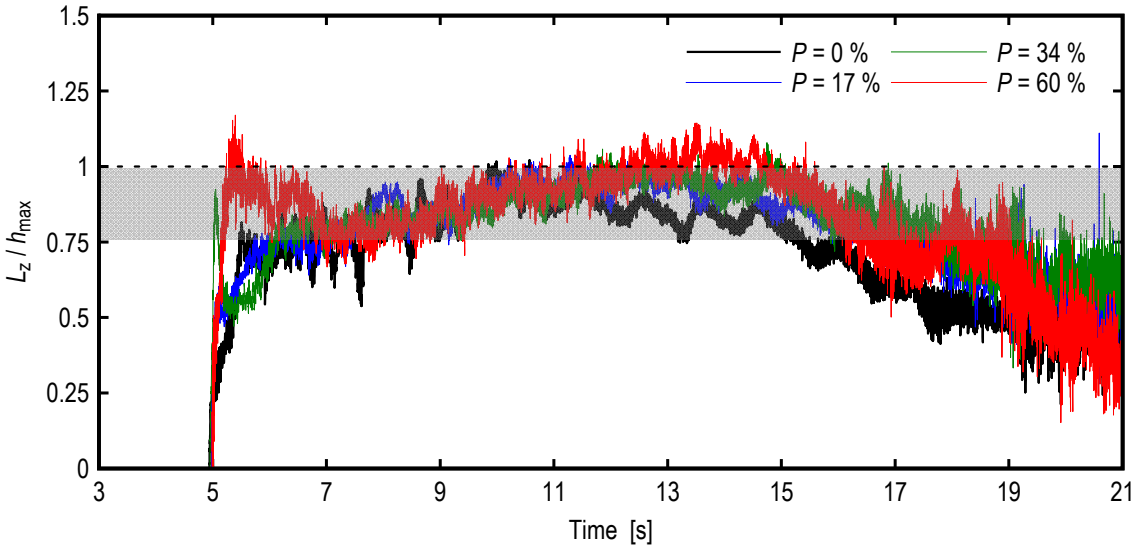

Figure 9. Lever arm, L_z computed as the ratio M_y/F_x for various porosity values.

5.3 Vertical Forces

Along with horizontal forces, **vertical forces F_z** played an important role in guaranteeing the survival of the structure. Two main components can be recognized: buoyancy, $F_{z,B}$ and the gravitational weight of water $F_{z,g}$. In the chosen reference system, the $F_{z,B}$ had to be considered negative, and $F_{z,g}$ positive. Being their signs opposites, the total force at the foundation is the algebraic sum of both components, as shown in Eq. [6]:

$$F_z = F_{z,B} + F_{z,g} \quad [6]$$

As the process was highly unsteady and the upstream water level continuously varied, the isolation of each component is hard to compute. The total force measured by the instrument is presented in Figure 10 for structures with various openings, along with the weight of water without the structure (P = 100%),

corresponding to the weight of the propagating surge. The maximum values of F_z are presented in Figure 8 as a function of *P.*

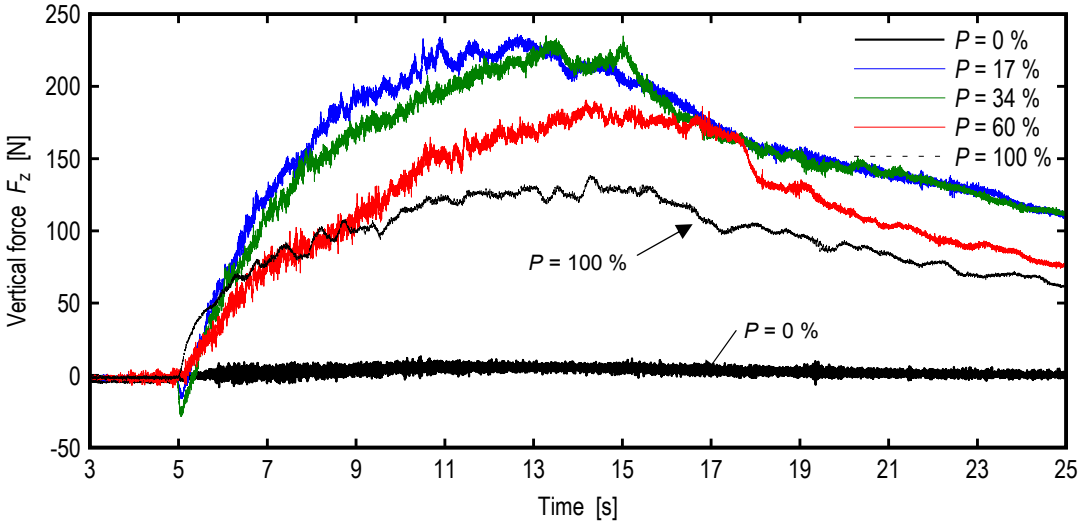

Figure 10. Time history of the total vertical forces, F_z measured for various porosity configurations.

For the impervious scenario, the absence of overflow above the structure resulted in vertical forces F_z close to zero, whereas for porous configurations the weight of the water flowing through the structure was obtained. One can notice that for porosities between 17 and 34 %, similar behaviours were observed, whereas for larger porosity values, smaller vertical forces were recorded. This was probably attributed to the "*accumulation*" of water upstream and inside the structure: in fact larger openings can facilitate the flow through the building and reduce the vertical load. The upper limit was represented by the scenario without structure (P = 100 %) showing lesser values if compared to the scenarios with the obstruction.

An initial uplift of the structure was observed for P = 17 and 34 %, attributed to the initial step encountered by the incoming wave, forcing the flow to deviate in the vertical direction and pushing the structure upward (Figure 6). The uplift did not occur for P = 60 % since the structure bottom was located at the same level as the channel. Similar results were previously discussed by Hartana and Murakami (2015).

6 CONCLUSIONS

Tsunamis, impulse waves and the sudden collapse of a dam are rare but catastrophic events, characterized by high reconstruction costs and important human losses. Some events that took place in the last decade showed that measures could be taken to limit devastation and reduce reconstruction costs. Furthermore post-event field trips showed that some structures behaved better than others and that openings seemed to reduce the forces applied to the structures.

The purpose of this experimental study is to reproduce the impact of a dry bed surge against a residential house commonly found in coastal areas. The wave was produced through a vertical release technique and the surge propagated on a smooth horizontal channel with a length of 15.5 m and a width of 1.4 m. The structure was simulated with a 0.3 m aluminum cube with two internal slabs representing the floors. The cubes were designed to be completely rigid, ensuring that the structure's response could be neglected. Wave height and velocity are measured through 7 Ultrasonic distance Sensors located along the channel.

All tested scenarios visually produced high splashes and similar run-up heights up to twice the building heights. For the configurations with openings, the incoming surge is able to flow through the structure resulting into lower upstream water depths.

The structure was assembled over a Dynamometric Force Plate allowing to measure total forces and momentum with an acquisition frequency of 1 kHz. Porosity values of 0 % (impervious), 17 %, 34 % and 60 % were systematically tested for one wave with identical release conditions. For the impervious structure, the **horizontal forces** in the flow direction showed no initial overshot and the process was considered quasi-steady due to the long period of the incoming surge. Findings showed a good agreement with the classical drag equation computed with the momentum flux hV_m^2 (Eq. [3]) using the wave height without the structure and the depth-averaged profile velocity behind the wave front. For the structures with openings a reduction of the horizontal force was systematically measured. Furthermore, a less steep increase in the force was noted for the porous configurations, resulting into a lower impulse transferred to the structure. The reduction in horizontal force was shown to be linearly proportional to the porosity values. The application point of the horizontal force was between 75 and 100 % of the wave height measured without the structure, independently of the geometry. Vertical forces represented the sum of both buoyancy and the gravitational weight of water.

An initial uplift was recorded only for the geometries with a vertical step deviating the incoming surge upward. The highest load in the vertical direction were recorded for porosities between 17 and 34 %.

These preliminary tests clearly showed the efficiency of building porosity in the reduction of the hydrodynamic load, pointing out the importance of its estimation for a safer design of coastal structures subjected to tsunami and impulse wave hazards.

ACKNOWLEDGEMENTS

The research reported herein is funded by the Swiss National Science Foundation SNSF (grants 200021_149112/1 and 200021_149112/2). The contribution and support of Prof. Anton Schleiss and Dr. Michael Pfister (Laboratory of Hydraulic Constructions (LCH), Ecole Polytechnique Fédérale de Lausanne (EPFL), Switzerland) are also acknowledged.

NOTATIONS

A_o	opened surface of the structure [m^2]
B	building width and height [m]
C_D	drag coefficient [-]
C_R	resistance coefficient [-]
d_0	equivalent impoundment depth [m]
f	Darcy-Weissbach friction factor
F_x	total Horizontal Force [N]
$F_{x,D}$	hydrodynamic force computed using V_m [N]
$F_{x,max}$	maximum horizontal force [N]
$F_{x,h}$	hydrostatic force computed with wave height (h) [N]
$F_{x,H}$	hydrostatic force computed with run-up height (H) [N]
F_z	total Vertical Force [N]
$F_{z,B}$	buoyancy [N]
$F_{z,g}$	gravitational weight of water [N]
$F_{z,max}$	maximum total vertical force [N]
g	gravity constant [m/s^2]
h	wave height without the structure [m]
h_{max}	maximum wave height without the structure [m]
H	run-up height with the structure [m]
H_{max}	maximum run-up height with the structure [m]
k	building stiffness [N/m]
L_z	lever arm [m]
M	momentum flux per unit width $M = hv^2$ [m^3/s^2]
M_y	moment around the y axis [Nm]
P	building surface porosity [%]
t	time [s]
U	wave front celerity [m/s]
v	flow velocity [m/s]
V_m	depth-averaged wave profile velocity [m/s]
x	streamwise coordinate [m]
y	transversal coordinate [m]
z	vertical coordinate [m]
β	blockage ration defined as $\beta = W/B$ [-]
ρ	water density [kg/m^3]

REFERENCES

Arnason, H., Petroff, C. & Yeh, H. (2009). Tsunami Bore Impingement onto a Vertical Column. *Journal of Disaster Research*, 4(6), 391-403.

CCH (2000). City and County of Honolulu Building Code (CCH). *Department of Planning and Permitting of Honolulu Hawaii*, Chapter 16, Article 11.

Chanson, H. (2006). Tsunami Surges on Dry Coastal Plains: Application of Dam Break Wave Equations. *Coastal Engineering Journal*, 48(4), 355-370.

Chanson, H., Aoki, S. & Maruyama, M. (2002). Unsteady Air Bubble Entrainment and Detrainment at a Plunging Breaker: Dominant Time Scales and Similarity of Water Level Variations. *Coastal Engineering*, 46(2), 139–157.

Chinnarasri, C., Thanasisathit, N., Ruangrassamee, A., Weesakul, S. & Lukkunaprasit, P. (2013). The Impact of Tsunami-Induced Bores on Buildings, *Proceedings of the ICE-Maritime Engineering*, 166(1), 14–24.

Chock, G., Robertson, I., Kriebel, D., Francis, M. & Nistor, I. (2012). Tohoku Japan tsunami of March 11, 2011 – Performance of structures. *American Society of Civil Engineers (ASCE)*.

Cross, R. (1967). Tsunami Surge Forces, *Journal of the Waterways and Harbors Division*, 93(4), 201–231.

FEMA 55 (2000). Coastal Construction Manual. *Federal Emergency Management Agency*, Washington DC, USA.

Hartana, & Murakami, K. (2015). Numerical and Experimental Simulation of Two-Phase Tsunami Flow Through Buildings with Openings, *Journal of Earthquake and Tsunami*, 9(3) (2015), 1550007, 15 pages.

Lukkunaprasit, P., Ruangrassamee, A. & Thanasisathit, N. (2009a). Tsunami loading on buildings with openings, *Science of Tsunami Hazards*, 28(5), 303.

Lukkunaprasit, P., Thanasisathit, N. & Yeh, H. (2009b). Experimental Verification of FEMA P646 Tsunami Loading, *Journal of Disaster Research*, 4(6), 410-418.

Madsen, P., Fuhrman, D. & Schäffer, H. (2008). On the Solitary Wave Paradigm for Tsunamis. *Journal of Geophysical Research: Oceans*, 113(C12) 1978–2012.

Meile, T., Boillat, J.L. & Schleiss, A.J. (2013). Propagation of Surge Waves in Channels with Large-Scale Bank Roughness. *Journal of Hydraulic Research*, 51(2), 195-202.

Nistor, I., Palermo, D., Nouri, Y., Murty, T. & Saatcioglu, M. (2009). Tsunami-Induced Forces on Structures. *Handbook of Coastal and Ocean Engineering*. Singapore, World Scientific, 261-286.

Nouri, Y., Nistor, I., Palermo, D. & Cornett, A. (2010). Experimental Investigation of The Tsunami Impact on Free-Standing Structures, *Coastal Engineering Journal*, JSCE, World Scientific, 52(1), 43-70.

Ramsden, J.D. (1996). Forces on a Vertical Wall due to Long Waves, Bores, and Dry-Bed Surges. *Journal of waterway, port, coastal, and ocean engineering,* 122(3), 134-141.

Thusyanthan, N. & Madabhushi, S. (2008). Tsunami Wave Loading on Coastal Houses: A Model Approach, *Proceedings of the ICE-Civil Engineering*, 161(2), 77-86.

Van de Lindt, J., Gupta, R., Garcia, R. & Wilson, J. (2009). Tsunami Bore Forces on a Compliant Residential Building Model, *Engineering Structures*, 31(11), 2534-2539.

Wüthrich, D., Pfister, M., Nistor, I. & Schleiss, A.J. (2017). Experimental Study of Tsunami-like Waves on Dry and Wet Bed Generated with A Vertical Release Technique. *Journal of Waterway, Port, Coastal, and Ocean Engineering*. (under review)

Wüthrich, D., Pfister, M. & Schleiss, A.J. (2016). Example of Wave Impact on a Residential House. *Proceedings of the 4th IAHR Europe Congress*, Liege, Belgium, 27-29 July 2016.

Yeh, H. (2007). Design Tsunami Forces for Onshore structures. *Journal of Disaster Research*, 2(6), 531-536.

Yeh, H., Liu, P. & Synolakis, C. (1996). Long-Wave Run-Up Models, *World Scientific Publishing Co*., Singapore, 403.

